Egypt. J. Chem. **Vol. 64,** No. 2 pp. 807 - 823 (2021)

Egyptian Journal of Chemistry

http://ejchem.journals.ekb.eg/

Electrochemical Behaviour of Two Dyes as Corrosion Inhibitors for Carbon Steel in Acid Medium and Studying Their Biological Activities by Practical and Theoretical Aspects

Ahmed A. El-Sonbaty[a,*], Ahmed A. Al-Sarawy[a], Mostafa A. Diab[b], Mahmoud H. Mahmoud[a]

[a] *Mathematical and Physical Engineering Department, Faculty of Engineering, Mansoura University, El-Mansoura, Egypt*

[b] *Chemistry Department, Faculty of Science, Damietta University, Egypt*

Abstract

The inhibitive action of azo dye aminophenol derivatives, namely 6-(4-benzenesulfonic acid azo)-3-aminophenol (compound (1)) and 4-(2,3-dimethyl-1-phenylpyrazol-5-one azo)-3-aminophenol (compound (2)) against the corrosion of C-steel in 2 M HCl solution using Tafel polarisation, surface morphology, electrochemical impedance spectroscopy and electrochemical frequency modulation techniques. The inhibition efficiency increased with increasing inhibitor concentrations and decreased with increasing temperature. Tafel polarization curves showed that the corrosion rate was decreased with increasing compounds concentration into HCl solution. Inhibition efficiency values obtained from various methods employed were in reasonable agreement. It was found that the order of percentage IE of these investigated compounds obey the following order: compound (2) > compound (1). In addition, the antimicrobial and antifungal activities of the aminophenol derivatives compounds (1 and 2) and comparing them with the standard antibacterial and antifungal drugs were described. The results showed that the compound (2) is very good antibacterial agents against Bacillus subtilis and Staphylococcus aureus. The compound (2) is more active than the compound (1) and penicillin G against Bacillus subtilis and Staphylococcus aureus. It was found that the compound (2) is more active than penicillin G which is used as the antibacterial standard drug against Enterobacter sp. and Klebsiella pneumoniae. Molecular docking was used to predict the binding between aminophenol derivatives compounds (1 and 2) and the receptors of the crystal structure of Staphylococcus aureus (3q8u) and the crystal structure of Escherichia coli (3t88). The compound (2) showed best interaction with receptor of Staphylococcus aureus (3q8u) than the compound (1).

*Keywords***:** Surface Morphology; Tafel polarization; Corrosion inhibition; SEM–EDX; Molecular docking; Antimicrobial activity.

Introduction

C-Steel is well known as an excellent mechanical and low cost corrosion inhibitor, and therefore it can be used in a wide range of industrial applications. It usually used in marine applications, chemical processing, drums, heat exchanger, tanks, petroleum production and refining, construction and metal processing equipment. Acid solutions are generally used for the removal of rust, during pickling, industrial cleaning and oil well acidizing which leads to corrosive attack on C-steel. Therefore, the uses of corrosion inhibitors aim to minimize or prevent corrosion, especially in acidic media, from occurring and protection of unexpected metal dissolution and acid consumption [1].

Organic corrosion inhibitors containing O, N, or S atoms and heterocyclic structures can significantly reduce the occurrence of corrosion with the addition of only very small amounts and consider more efficient inhibitors [2-4]. Hetero atoms, such as nitrogen, oxygen and sulfur adsorbed on the metal surface are blocking the active sites and generating a physical

*Corresponding author e-mail: aaelsonbaty@hotmail.com.; (Ahmed A. El-Sonbaty).
Receive Date: 02 September 2020, Revise Date: 23 September 2020, Accept Date: 04 October 2020
DOI: 10.21608/EJCHEM.2020.41579.2842

barrier to reduce the transport of corrosive species to the surface of the metal [5-7]. Adsorption is affected by the nature, surface and the chemical structure of inhibitors charge of the metal [8-10].

The scope of the present work is to study the corrosion inhibition effect and electrochemical behavior of newly synthesized aminophenol derivatives compounds (1 and 2) for C-steel in 2 M hydrochloric acid solution by the Tafel polarization, electrochemical frequency modulation (EFM) and electrochemical impedance spectroscopy (EIS) techniques. The test coupon surfaces were analyzed using scanning electronic microscopy (SEM), revealed that the compounds under investigation form a protective film from corrosion on the C-steel surface in 2 M HCl and acts as a barrier to corrosive media. Molecular docking is used to predict the binding between aminophenol derivatives compounds (1 and 2) and the receptors of the crystal structure of *Staphylococcus aureus* (3q8u) and the crystal structure of *Escherichia coli* (3t88). Also, we describe the antimicrobial and antifungal activities of the aminophenol derivatives compounds (1 and 2) and comparing them with the standard antibacterial and antifungal drugs.

Experimental

Inhibitor preparation and characterization

The azo dye aminophenol derivatives compounds of 6-(4-benzenesulfonic acid azo)-3-aminophenol (Compound (1)) and 4-(2,3-dimethyl-1-phenylpyrazol-5-one azo)-3-aminophenol (Compound (2)) were prepared and characterized by various spectral techniques as described by El-Sonbati et al. [11]. The different azo dye aminophenol derivatives compounds are represented in Table S1.

Metal coupons composition and medium

The wt. % composition of C-steel used in corrosion measurements is 0.20 C, 0.53 Mn, 0.3 Si, 0.055S, 0.045P, Fe balance. 2 M HCl was prepared by dilution of HCl (BDH grade, 37%) with double distilled water.

Techniques utilized for measurements

All the experiments were carried out by using ultra circulating thermostat at 25 ^{o}C and the solutions were not deaerated. The curves of potentiodynamic current potential were registered by changing the potential of electrode from -500 to 500 mV automatically by using Potentiostate (Gamry PCI 300/4) with scanning rate 5 mVs^{-1} and for calculations with DC 105 software and with the aid of computer which as well registered and stored and saved the data in case of carbon steel. Before take place any experiment, the working electrode was polarized at potential of -1.5 V to reduce the pre-immersion oxide film for 20 minutes on the electrode surface.

Tafel polarization method

Tafel polarization method was carried out in thermostatic cell conventional assembly using three electrodes (a sheet of platinum as a counter electrode, saturated calomel electrode (SCE) and C-steel electrode of size 1 x 1 cm) and was utilized a Gamry Galvanost at/ZRA/ Potentiostat (model PCI 300/4). The potentiostatic diagrams were occurred from -5 to 5 V at a scan with rate 0.5 mVs^{-1} after reached to the steady state (30 minutes).

Electrochemical Frequency Modulation Technique (EFM)

EFM technique was used for the determination of the rate of corrosion at 30 ± 1 °C. It was performed by utilization of two different frequencies of 2.0 and 5.0 Hz. The intermodulation current responses form corrosion density ($i_{corr.}$) and harmonical intermodulation peaks of current are determined each 30 min. The larger peaks were used to measure the current, the Tafel slopes (β_a and β_c) and the causality factors (CF2 and CF3) [2,10].

Electrochemical impedance spectroscopy (EIS)

The circuit model of equivalent electrical was utilized for this system where R_{ct}= charge transfer resistance, R= resistor and R_s= resistance of solution, and C_{dl} = the capacitance of double layer. EIS300 software of Gamry applications was used for EIS measurement.

Surface morphology (SEM-EDX)

The C- steel analysis was dipped for three days in 2 M HCl with and without the investigated inhibitors. The morphology on the C-steel surface was carried out by using scanning electron microscopy (SEM) using JOEL, JSM-T20, Japan into the spectrometer (pw-1390) Philips.

Assay of antimicrobial activities

Agar well diffusion method [12-15] was used to assay the antimicrobial activity of the aminophenol derivatives compounds (1 and 2) at different concentrations (50, 100 and 150 µl) using dimethylformamide (DMF) as solvent. DMF was also tested as a control. The antibacterial activities against *Bacillus subtilis*, *Staphylococcus aureus*, *Bacillus cereus*, *Klebsiella pneumoniae*, *Escherichia coli*, *Pseudomonas* sp. and *Enterobacter* sp. were assayed on nutrient agar medium. The antifungal activities were assayed against *Aspergillus niger*, *Candida albicans and Fusarium oxysporum* using DOX agar medium. Wells (10 mm) were inoculated with the tested bacteria or fungi in in agar medium. Each tested compound (200 µl) was put in a well. The agar plates were kept at 4 °C for 30 min., then incubated them at 37 and 30 °C for bacteria and fungi, respectively. The standard drugs (penicillin and miconazole) were also tested in comparison with the compounds. The activities of antimicrobial were assayed by measuring diameters of the inhibition zones after 24 hours and 7 days for bacteria and fungi, respectively.

Analysis of molecular docking

The molecular docking of aminophenol derivatives compounds (1 and 2) was performed to different bacterial cell division proteins. In the study the actual docking process

in which the aminophenol derivatives (1 and 2) – protein pair-wise interaction energies are calculated using Docking Server [16-19]. The MMFF94 Force field was used to minimize the energy of aminophenol derivatives compounds (1 and 2) molecules using Docking Server. Gasteiger partial charges were added to the aminophenol derivatives compounds (1 and 2) atoms. Docking calculations were carried out on the receptor of crystal structure of *Staphylococcus aureus* (3q8u) and the receptor of crystal structure of *Escherichia coli* (3t88) proteins model. Essential hydrogen atoms, solvation parameters and Kollman united atom type charges were added with the aid of AutoDock tools [20-23].

Results and Discussion

Characterization of the compounds

The compounds (1 and 2) were prepared as described previously [11]. The structure of the formed compounds (Fig. 1) was established by elemental analyses, IR, ^{1}H NMR spectroscopes (Table S2) and X-Ray diffraction analysis.

The X-ray diffraction (XRD) pattern of the compound (1) is shown in Fig. 2. The XRD pattern of compound (1) shows many diffraction peaks which indicate the polycrystalline phase [24-26]. The lattice parameters (a, b, c, α, β and γ) and Miller indices (hkl) for compound (1) is estimated and listed in Table S3. The XRD pattern of compound (2) shows broad peaks indicate that compound (2) is a mixture of crystalline and amorphous phases [27,28].

Tafel polarization measurements

The effect of the addition of aminophenol derivatives on the corrosion rate of C-steel was investigated by Tafel polarization method. The changes in the polarization plots after the addition of aminophenol derivative inhibitors are usually utilized as the criteria as cathodic, anodic or mixed inhibitors [29]. Fig. 3 shows the plots of Tafel polarization for C-steel for different potion of compound (1) at 30 ºC. Same plot was given for other aminophenol derivative compounds. The cathodic curves shown in Fig. 3 give almost lines parallel indicating that the hydrogen atoms emptying the reaction lower, it's the activation being controlled by the addendum of organic compounds [30,31]. The kinetic parameters of corrosion potential (E_{corr}), inhibition efficiency values (% IE_p), corrosion current density (i_{corr}), anodic and cathodic Tafel slopes (β_a and β_c) were obtained by the data of Tafel plots and given in Table 1. In addition to the study of the all concentrations result showed the following:

- A decrease in the corrosion rate leads to a decrease in the current density (icorr).
- The existence of an improvement on the surface of coverage leads to increasing in the values of % IEp.
- No shift was observed in the data of potential of corrosion (Ecorr) with estimate to the blank.
- The slopes of the anodic and cathodic Tafel lines (β_a and β_c) include nearly unchanged upon appending of aminophenol derivatives compounds (1 and 2), giving improving to almost parallel cathodic plots results and a nearly parallel set of anodic lines.

The inhibition efficiency was measured using the equation (1):

$$\%IE_p=[(i^o_{corr}-i_{corr})/i^o_{corr}]x100 \quad \ldots\ldots\ldots\ldots \quad (1)$$

where i^o_{corr} and i_{corr} = current corrosion densities without and with aminophenol derivatives inhibitors, respectively.

So, the adsorbed of aminophenol derivatives compounds (1 and 2) inhibitors blocking the sites of active for both anodic and cathodic methods. The adsorbed aminophenol derivatives compounds (1 and 2) inhibitors lower the area of corrosion surface without impressive the mechanism or technique of corrosion process on C-steel in 2 Molar HCl solution. The efficiency of inhibition of the inhibitors of aminophenol derivatives compounds (1 and 2) as the following the arrangement: Compound (2) > Compound (1).

EFM methods

Figure 4 represents the EFM spectra for C-steel with and without different concentrations of compound (1). Similar diagrams were given in compound (2). Two different the values of EFM were used two various models:

i- The activation of model.

ii- The complete diffusion control of the cathodic reaction

For the activation of model, assuming that the potential of corrosion does not change because of the polarization of the working electrode, a set of three non-linear equations had been used [32]. From EFM, the kinetic parameters like as the corrosion density current (i_{corr}), the causality factors (CF-2 & CF-3) and Tafel slopes (β_c and β_a) are listed in Table 2. It was found that the values of the protection efficiency (%IE) increased by through increasing the concentrations of the aminophenol derivatives compounds (1 and 2) as inhibitors. The factors of causality are found to be near to the data of theoretical, this indicates that the calculated data are good. The % IE (inhibition efficiencies) is calculated by through the Eq. (2):

$$\%\,IE_{EFM} = 100 \times [\,1 - (\,i_{corr} / i^o_{corr}\,)\,] \ldots\ldots \quad (2)$$

Where i^o_{corr} is corrosion current densities without the inhibitors and i_{corr} is corrosion current densities with the inhibitors. The protective efficiency showed from the EFM experiment is in the following order: (2) > (1).

EIS measurements

Fig. 5 shows the Nyquist and Bode plots (a and 2, respectively) observed from open-circuit potential without and with the addition of different concentrations of aminophenol derivatives at 30 ± 1 ºC. The increasing in the value of size of the loop capacitive with the addition of vloume of aminophenol derivatives compounds (1 and 2) as inhibitors leading to a barrier progressively forms on the C-steel surface. The improving in the size of loop capacitive with regard to the steady inhibitor dose (Fig. 5a), as the following order: compound (2) > compound (1), indicating the inhibitive influence of compound (2). Bode curves (Fig. 5b), shows that the increase in impedance by increasing the concentration of aminophenol derivative compounds [33-36]. Also Bode curve lead to an increase in the angle phase of shift, indicating the effect of adsorbed aminophenol compounds as inhibitors on the surface of C-steel. The dispersion of frequency is due to the variation from ideal semicircle [37]. Fig. S1 appear a transfer reaction of single charge and which fits well with previously mentioned of data

experimental. Equation 3 was used for measuring C_{dl} of a circuit containing a CPE parameters (n and Y_0) [38]:

$$C_{dl} = Y_0\omega^{n-1} / \sin [n (\pi/2)] \ldots\ldots (3)$$

whereY_0 is the magnitude of the CPE, f_{max} is the frequency at which the imaginary component of the impedance is maximal and ω is the $2\pi f_{max}$. The curves of Nyquist for the corrosion process were fundamentally controlled on charged-transfer [39]. EIS data in Table 3 showed that the R_{ct} data increased and the C_{dl} data decreased by through increasing the concentrations of aminophenol derivatives compounds (1 and 2) as inhibitors. This is attributed to the gradual water molecules by the adsorption of the molecules of aminophenol derivatives compounds (1 and 2) as replacement of inhibitors on the surface of C- steel, lowering the extent of reaction of dissolution. The increased values of R_{ct}, are generally, combine with lower corroding system, while the lower values of C_{dl} can be obtained from the low of the constant of local dielectric and /or from the increase of electrical double layer thickness [40]. It seems that the aminophenol compounds (1 and 2) inhibitors molecules function by through adsorption in the solution/ interface of the metal.

The % E inhibition efficiency is measured by using the equation (4) [8,41]:

$$\% E = 100 \times \theta = [1-(R^{\circ}_{ct}/R_{ct})] \ldots\ldots (4)$$

where, R^{o}_{ct} is the charge transfer resistance in the absence of inhibitor and R_{ct} is the charge transfer resistance in the presence of inhibitor. The order of the values of % E inhibition efficiency of the investigated aminophenol derivatives compounds (1 and 2) is the same as in the measurements of Tafel polarization (2 >1).

SEM investigation and EDX analysis

SEM images of C-steel are shown in Fig. S2 (before and after corrosion). SEM images give a variation between the microstructures of surface on C-steel in 2 M HCl before corrosion step and after corrosion step with and without of 11 x 10^{-6} M of aminophenol derivatives compounds (1 and 2) as inhibitors (1 and 2) (Table 4). The images of SEM show that the addition of aminophenol derivatives compounds (1 and 2) as inhibitors to HCl has important effect on the morphology of C-steel. The protective film of inhibitor at the electrode surface was further confirmed by SEM images of the metal surface. As well, both the experiments of SEM and EDX were used to study the images of morphological for surface of C-steel exposed to the 2 Molar HCl solution with and without the addition of the aminophenol derivatives compounds which optimum concentration (Figs. S2 and 6, respectively). There was a remarkable improvement in the morphology of the surface of C-steel when treated with the inhibitor attributed to the formation of an adsorbed protective film at the sample surface of the inhibitor. Or, it may be because of the involvement of the molecules of inhibitor in the interaction with the reaction sites of surface of C-steel, this resulting in a decrease in the connect between C-steel and sequentially exhibited perfect inhibition effect and the aggressive medium [42].

The EDX spectra (Figure 6) were used to calculate the elements present on the surface of C-steel. The presence of a nitrogen atoms and carbon atoms in the spectra of EDX for the surface of C-steel due to the samples immersed in solutions containing the 11×10^{-6} Molar of the aminophenol derivatives compounds (1 and 2) as inhibitors for three days, indicates that the molecules of aminophenol derivatives compounds (1 and 2) are adsorbed on the of C-steel surface and protecting it against the corrosion..

Mechanism of Inhibition of Corrosion

From electrochemical techniques, it was found that the inhibition efficiency of C-steel in 2M HCl solution in presence of aminophenol derivatives compounds (1 and 2) depends on concentration, nature of metal, the mode of adsorption of the inhibitors and surface conditions. There is a decrease of the corrosion rate and corrosion current with increasing in concentration of the inhibitors. In addition, the shift in Tafel lines to higher potential regions was observed. Therefore, it seems that the % inhibition efficiency depends on the number of active centers of adsorption at the electrode solution interface in the molecule depends on the affinity of the metal towards the π-electron clouds of the ring system and their charge density. Polar character of substituents in the changing part of the inhibitor molecule seems to have a prominent effect on the electron charge density of the molecule. The transfer ormotion of lone pairs of electrons on the nitrogen atoms to the C-steel surface to form a coordinate type of linkage is favored by the presence of a vacant orbital in iron atom of low energy. C and Fe metals have a greater affinity towards aromatic moieties were found to adsorb benzene rings in a flat orientation. The order of decreasing the inhibition efficiency of the investigated aminophenol inhibitors in the corrosive solution was as follows: compound (2) > compound (1). Excellent inhibition efficiency is found in compound (2) than compound (1) due to its larger molecular size (323 and 293, respectively) which facilitate better surface coverage and larger molecular area. Apart from this it was found that the adsorption occurs through seven active atoms centers where 2 oxygen atoms and 5 nitrogen atoms in compound (2), while compound (1) was found to possess less inhibition efficiency due to its eight active atoms centers where 4 oxygen atoms, 1 sulphur atom and 3 nitrogen atoms

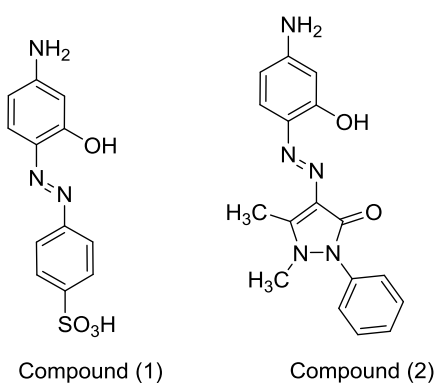

Fig. 1. The structures of compounds (1 and 2).

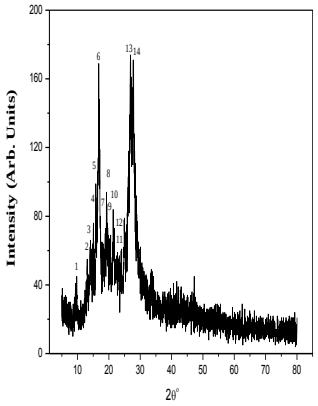

Fig. 2. X-ray diffraction patterns of compound (1).

Table 1: The effect of concentration of the compounds (1 and 2) on the corrosion current density (i_{corr}), the free corrosion potential (E_{corr}), inhibition efficiency (% IE), Tafel slopes (βa & βc) and degree of surface coverage of the corrosion of C-steel for compounds (1 and 2) in 2 M HCl at 30 ± 1 ºC.

Comp.	Conc., M.	- E_{corr} (mV vs. SCE)	$i_{corr} \times 10^{-4}$ (μA cm^{-2})	$\beta_a \times 10^{-3}$ (mV dec^{-1})	$\beta_c \times 10^{-3}$ (mV dec^{-1})	θ	% IE
Blank	Blank	487	8.18	124.2	125.9	----	-----
	$1x10^{-6}$	484	6.46	126.0	89.5	0.210	21.0
	$3x10^{-6}$	465	5.94	37.8	30.7	0.273	27.3
(1)	$5 x10^{-6}$	440	5.57	81.0	92.9	0.319	31.9
	$7x10^{-6}$	452	5.20	95.4	69.9	0.364	36.4
	$9x10^{-6}$	441	5.04	108.3	87.0	0.383	38.3
	$11x10^{-6}$	431	4.50	86.8	145.4	0.449	44.9
	$1x10^{-6}$	446	4.43	81.1	105.5	0.458	45.8
	$3x10^{-6}$	464	4.31	184.9	177.9	0.473	47.3
(2)	$5 x10^{-6}$	453	1.91	206.0	127.0	0.766	76.6
	$7x10^{-6}$	438	1.88	47.1	46.6	0.770	77.0
	$9x10^{-6}$	449	1.12	36.7	30.5	0.863	86.3
	$11x10^{-6}$	473	1.04	125.9	239.5	0.872	87.2

Table 2: Electrochemical kinetic parameters obtained by EFM technique for C- steel in 2 M HCl without and with various concentrations of investigated compounds at 30 ± 1 ºC.

Comp.	Conc., M.	icorr (μA cm-2)	βa × 10-3 (mV dec-1)	βc × 10-3 (mV dec-1)	CF-2	CF-3	C.R	θ	%IE
Blank	Blank	520.4	90.74	112.2	1.93	3.01	237.8	-----	------
	1x10-6	257.4	27.00	31.4	2.19	3.06	117.6	0.505	50.5
(1)	3x10-6	257.0	28.12	29.7	1.79	3.08	117.4	0.506	50.6
	5 x10-6	256.4	28.06	29.5	1.76	3.04	117.2	0.507	50.7
	7x10-6	252.0	27.37	28.7	1.95	3.30	115.2	0.516	51.6

	9x10-6	247.3	26.57	27.9	1.93	3.07	113.0	0.525	52.5
	11x10-6	243.7	26.02	27.3	1.91	3.15	111.4	0.532	53.2
	1x10-6	243.0	25.51	27.7	1.85	3.02	111.2	0.533	53.3
	3x10-6	242.0	25.45	27.6	1.80	3.14	111.0	0.534	53.4
(2)	5 x10-6	240.7	25.42	26.8	1.92	3.05	110.0	0.537	53.7
	7x10-6	239.3	25.39	26.4	1.93	2.83	109.4	0.540	54.0
	9x10-6	199.2	97.85	104.1	2.03	3.04	91.0	0.617	61.7
	11x10-6	119.9	89.48	95.0	1.99	3.15	54.8	0.769	76.9

Table 3: Electrochemical kinetic parameters obtained from EIS technique for C- steel in 2 M HCl in the absence and presence of different concentrations of investigated compounds at 30 ± 1 °C

Comp.	Conc., M.	R_S (Ω cm^2)	$Y_{o} \times 10^{-3}$ ($\mu\Omega^{-1}s^{n}$)	$n \times 10^{-3}$	R_{ct} (Ω cm^2)	$C_{dl} \times 10^{-4}$ (μFcm^{-2})	θ	%IE
	Blank	612.8	638.7	878.7	10.82	8.31	-----	------
	$1x10^{-6}$	817.5	313.7	863.5	15.57	8.08	0.305	30.5
	$3x10^{-6}$	797.3	178.0	761.8	16.33	6.10	0.337	33.7
	$5 x10^{-6}$	653.0	166.4	779.4	17.37	5.88	0.377	37.7
(1)	$7x10^{-6}$	824.0	975.1	829.7	18.89	4.29	0.427	42.7
	$9x10^{-6}$	744.8	726.1	876.3	20.82	4.01	0.480	48.0
	$11x10^{-6}$	210.4	202.7	760.3	29.26	3.21	0.630	63.0
	$1x10^{-6}$	644.5	403.3	893.0	32.25	2.39	0.664	66.4
	$3x10^{-6}$	791.0	319.0	880.3	41.44	1.81	0.739	73.9
	$5 x10^{-6}$	738.9	327.7	874.6	49.00	1.77	0.779	77.9
(2)	$7x10^{-6}$	732.2	286.9	856.1	95.86	1.56	0.887	88.7
	$9x10^{-6}$	825.5	243.1	863.7	101.0	1.36	0.893	89.3
	$11x10^{-6}$	687.4	128.7	896.8	136.7	1.35	0.921	92.1

Table 4
Surface composition (weight %) of C-steel for compounds (1 and 2) without and in presence inhibitor of 11x 10 $^{-6}$ M in 2 M HCl solution after immersion for 3 days.

(Mass %)	C	O	Al	Si	Cr	Mn	Fe	Tb
Pure Sample	6.78	---	0.29	0.28	0.22	0.47	87.53	4.43
Blank	8.67	17.84	----	----	----	0.39	68,85	4.25
Compound (1)	10.48	13.40	0.30	0.22	0.18	0.41	70.90	4.11
Compound (2)	12.03	8.33	----	----	----	0.41	74.87	4.36

Antimicrobial activity of the compounds

Antibacterial and antifungal activities of aminophenol derivatives compounds (1 and 2) were tested against three local gram-positive bacteria (*Bacillus subtilis, Staphylococcus aureus and Bacillus cereus*) and four local gram-negative bacteria (*Klebsiella pneumoniae, Escherichia coli, Pseudomonas* sp. and *Enterobacter* sp.) as well as antifungal activities were determined against *Fusarium oxysporum, Aspergillus niger* and *Candida albicans* and the results were recorded in Tables 5 and 6 and shown in Figs. 7, 8 and S3. Aminophenol derivatives compounds (1 and 2) have no antibacterial activity against *Bacillus cereus*. Also compound (1) has no antibacterial activity against *Enterobacter* sp. and compound (2) has no antibacterial activity against *Escherichia coli*. The compound (2) has antibacterial activity against *Bacillus subtilis* (inhibition zone = 15, 18 and 20 mm at concentrations = 50, 100 and 150 µg/ml, respectively) and the compound (1) has antibacterial activity against *Bacillus subtilis* (inhibition zone = 11, 15 and 17 mm at concentrations = 50, 100 and 150 µg/ml, respectively). The compound (2) has antibacterial activity against *Staphylococcus aureus* (inhibition zone = 17, 19 and 22 mm at concentrations = 50, 100 and 150 µg/ml,) and the compound (1) has antibacterial activity against *Staphylococcus aureus* (inhibition zone = 15, 18 and 21 mm at concentrations = 50, 100 and 150 µg/ml, respectively) as shown in Fig. 4. The compound (2) has no antibacterial activity against *Escherichia coli* but compound (1) has antibacterial activity against *Escherichia coli* (inhibition zone = 11, 14 and 16 mm at concentrations = 50, 100 and 150 µg/ml, respectively). The compound (2) has antibacterial activity against *Klebsiella pneumoniae* (inhibition zone = 7, 13 and 20 mm at concentrations = 50, 100 and 150 µg/ml, respectively) and the compound (1) has antibacterial activity against *Klebsiella pneumoniae* (inhibition zone = 15, 18 and 23 mm at concentrations = 50, 100 and 150 µg/ml, respectively) as shown in Fig. S5. The compound (2) has antibacterial activity against *Pseudomonas* sp. (inhibition zone = 14, 18 and 20 mm at concentrations = 50, 100 and 150 µg/ml,) and the compound (1) has antibacterial activity against *Pseudomonas* sp. (inhibition zone = 21, 25 and 27 mm at concentrations = 50, 100 and 150 µg/ml, respectively) as shown in Fig. S6. The compound (1) has no antibacterial activity against *Enterobacter* sp. but compound (2) has antibacterial activity against *Enterobacter* sp. (inhibition zone = 8, 11 and 15 mm at concentrations = 50, 100 and 150 µg/ml, respectively).
The results showed that the compound (2) is very good antibacterial agents against *Bacillus subtilis* and *Staphylococcus aureus* (Table 5). The compound (2) is more active than the compound (1) and penicillin G against *Bacillus subtilis* and *Staphylococcus aureus* (Table 5). As well as it was found that the compound (2) is more active than penicillin G which is used as the antibacterial standard drug against *Enterobacter* sp. and *Klebsiella pneumoniae*. The tested compound (2) showed very good antibacterial activity in comparison with penicillin G. Azo dye compounds usually showed antibacterial activities [13, 43-45].
The antifungal activity results of the aminophenol derivatives compounds (1 and 2) were investigated against *Fusarium oxysporum, Aspergillus niger* and *Candida albicans* and listed in Table 6. It was found that the compound (2) has neither antifungal nor anticandidal activities but the compound (1) has antifungal activity against *Aspergillus niger* (inhibition zone = 10, 15 and 21 mm at concentrations = 50 100 and 150 µg/ml, respectively), *Fusarium oxysporum* (inhibition zone = 13 and 18 mm at concentrations = 100 and 150 µg/ml, respectively) [12,46] and against *Candida albicans* (inhibition zone = 9, 14 and 18 mm at concentrations = 50, 100 and 150 µg/ml, respectively).

Molecular docking of the compounds The aminophenol derivatives compounds (1 and 2) generally bound to the receptors with higher affinity than their original compounds (1 and 2) (Tables 7 and 8). The molecular docking was used to reveal the interacting active residues with receptors, which was endorsed to interlink with phytochemical by the energies and interact surface area size [8,9,47-51]. The present results obtained from data showed that the molecular interactions of aminophenol derivatives compounds (1 and 2) with *Staphylococcus aureus* (3q8u) and *Escherichia coli* (3t88) as shown in Figs. 9 and 10 were mentioned in Tables 7 and 8, which indicates specific bonds and atoms involved in the docking.
The results of the molecular docking between aminophenol derivatives compounds (1 and 2) and receptors of *Staphylococcus aureus* (3q8u) and *Escherichia coli* (3t88) showed a possible arrangement between aminophenol derivatives compounds (1 and 2) and *S. aureus* (3q8u) receptor. The docking study showed a favorable interaction between aminophenol derivatives compounds (1 and 2) and the receptors as shown in Figs. S7 and S8 and the calculated energy is listed in Tables 7 and 8. According to the results obtained in this study, HB plot curve indicates that the aminophenol derivatives compounds (1 and 2) binds to the proteins with hydrogen bond interactions and decomposed interaction energies in kcal/mol were exist between aminophenol derivatives compounds (1 and 2) with *S. aureus* (3q8u) and *E. coli* (3t88) receptors as appear in Figure S9 and Figure S10 which showed curves of 2D of docking with aminophenol derivatives compounds (1-2).

The compound (2) showed best interaction with *Staphylococcus aureus* (3q8u) receptor than the compound (1).

Table 5: Antibacterial activities of the aminophenol derivatives compounds (1 and 2) in comparison with benzylpenicillin (penicillin G) as a standard drug. *The diameter of zones of inhibition (mm)

Compound	Concentration(µg/mL)	Gram-positive bacteria			Gram-negative bacteria			
		Bacillus cereus	*Bacillus subtilis*	*Staphylococcus aureus*	*Escherichia coli*	*Klebsiella pneumoniae*	*Pseudomonas* sp.	*Enterobacter* sp.
(1)	50	-ve	11 ± 0	15 ± 0	11 ± 0.03	15 ± 0	21 ± 0	-ve
	100	-ve	15 ± 0	18 ± 0.03	14 ± 0.03	18 ± 0	25 ± 0.03	-ve
	150	-ve	17 ± 0.03	21 ± 0	16 ± 0	23 ± 0	27 ± 0	-ve
(2)	50	-ve	15 ± 0	17 ± 0	-ve	7 ± 0	14 ± 0.03	8 ± 0
	100	-ve	18 ± 0.03	19 ± 0	-ve	13 ± 0	18 ± 0.14	11 ± 0
	150	-ve	20 ± 0.03	22 ± 0.03	-ve	20 ± 0	20 ± 0	15 ± 0
Penicillin G	50	11 ± 0	15 ± 0	10 ± 0	37 ± 0	-ve	12 ± 0	-ve
	100	13 ± 0.03	16 ± 0	11 ± 0	40 ± 0.06	-ve	15 ± 0.06	-ve
	150	16 ± 0.03	17 ± 0	16 ± 0.03	42 ± 0	-ve	22 ± 0	-ve

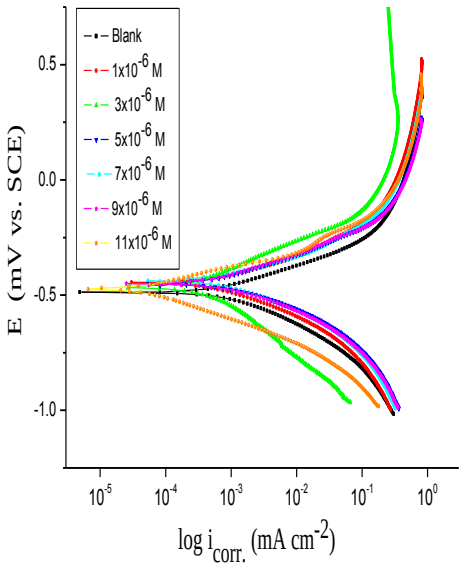

Fig. 3. Curves of potentiodynamic polarization of the corrosion of carbon steel in the absence and presence of different concentrations of compound (1) in 2 M HCl at 30 ± 1 ºC.

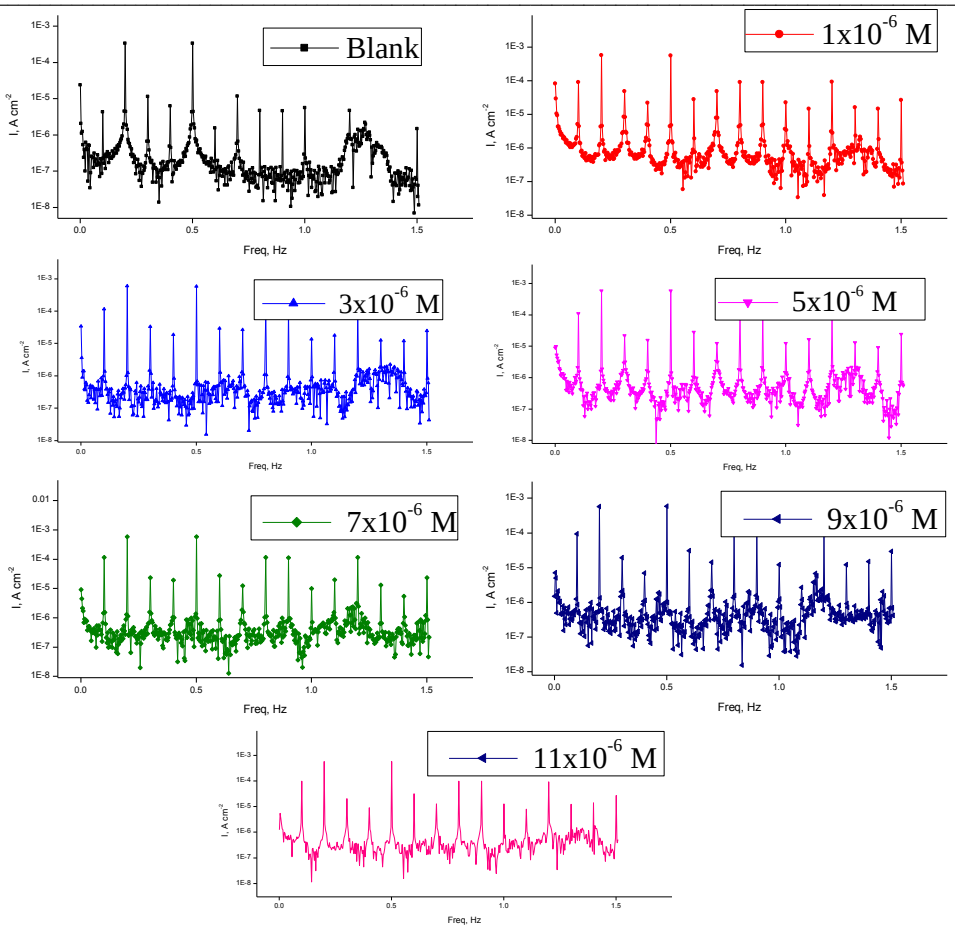

Fig. 4. The spectra of EFM of the corrosion of carbon steel in the absence and presence of different concentrations of compound (1) in 2 M HCl at 30 ± 1 ºC.

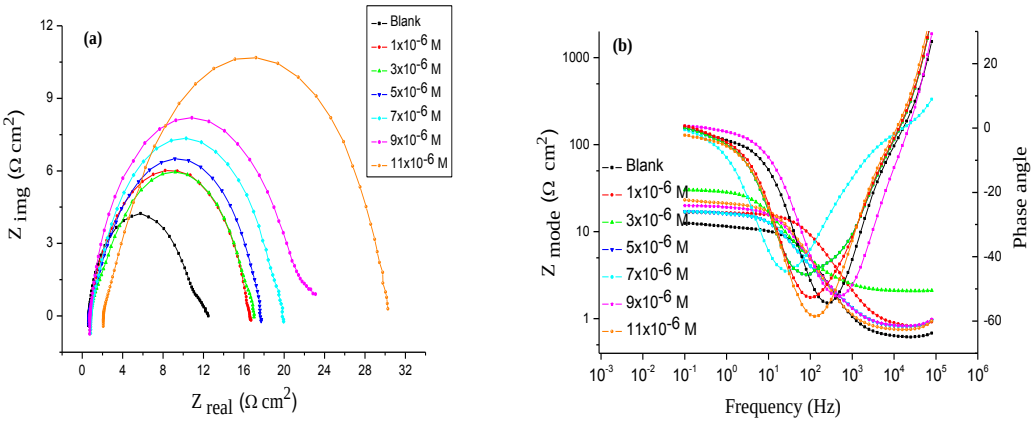

Fig. 5. (a) Plot of Nyquist and (b) plot of Bode of C- steel in absence and presence of different concentrations of compound (1) in 2 M HCl at 30 ± 1 ºC.

Pure sample

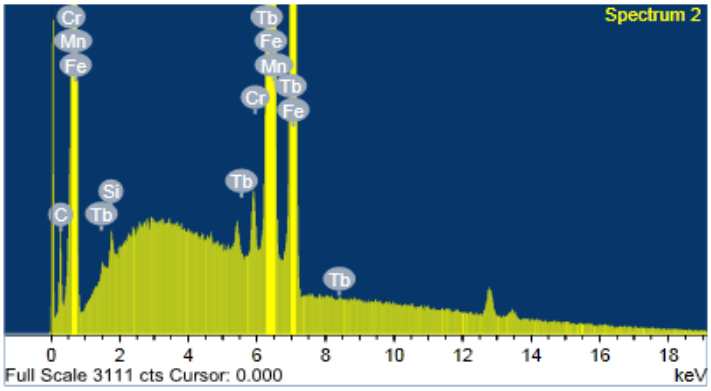

Blank

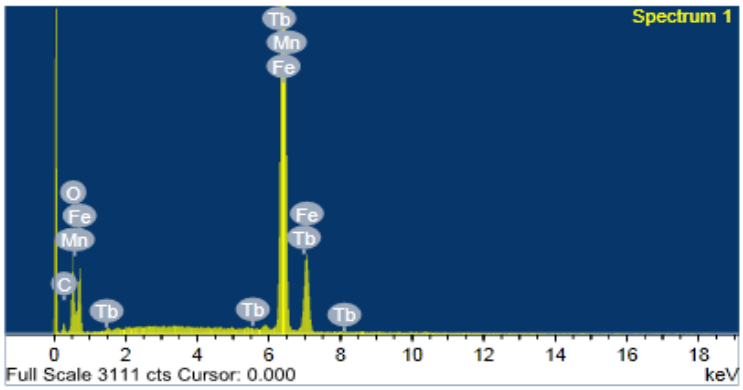

Compound (1)

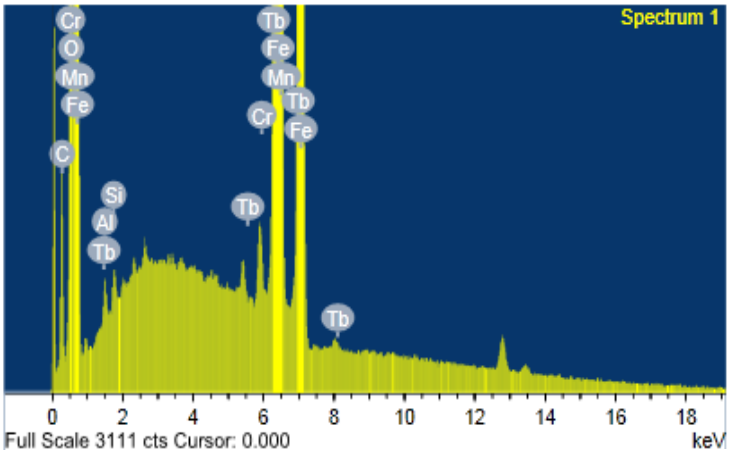

Compound (2)

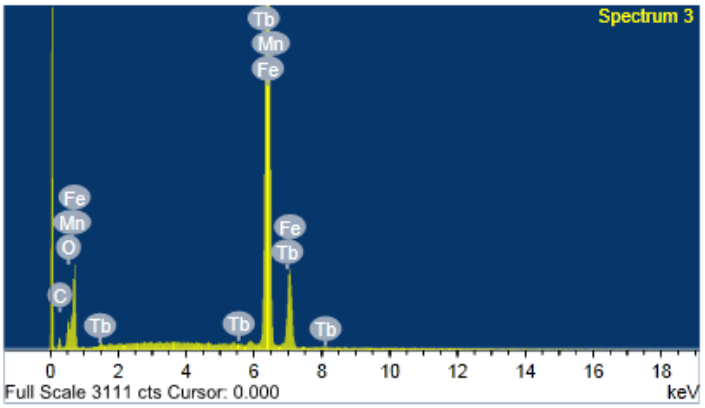

Fig. 6. EDS analysis of C-steel for compounds (1 and 2) without and in presence inhibitor of 11x 10 $^{-6}$ M in 2 M HCl solution after immersion for 3 days.

Table 6: Antifungal activities of the aminophenol derivatives compounds (1 and 2) in comparison with miconazole as a standard drug. *The diameter of zones of inhibition (mm).

Compound	Concentration µg/mL)(	*Aspergillus niger*	*Fusarium oxysporum*	*Candida albicans*
	50	10 ± 0.03	-ve	9 ± 0.03
(1)	100	15 ± 0	13 ± 0.03	14 ± 0
	150	21 ± 0	18 ± 0.03	18 ± 0
(2)	50	-ve	-ve	-ve
	100	-ve	-ve	-ve
	150	-ve	-ve	-ve
Miconazole	50	11 ± 0.03	11 ± 0	10 ± 0
	100	13 ± 0	13 ± 0.06	12 ± 0
	150	17 ± 0.06	14 ± 0.06	16 ± 0.06

Table 7: The values of energy obtained in docking calculations of aminophenol derivatives compounds (1 and 2) with receptor of *Staphylococcus aureus* (3q8u).

Compound	Est. Free Energy of Binding (kcal/mol)	Est. inhibition constant (K_i) (µM)	vdW+ bond+ desolv energy (kcal/mol)	Electrostatic Energy (kcal/mol)	Total intercooled Energy (kcal/mol)	Interact surface
(1)	-4.96	232.41	-6.15	-0.11	-6.26	607.150
(2)	-4.98	225.29	-6.51	-0.14	-6.65	676.888

Table 8: The values of energy obtained in docking calculations of aminophenol derivatives compounds (1 and 2) with receptor of *Escherichia coli* (3t88).

Compound	Est. Free Energy of Binding (kcal/mol)	Est. inhibition constant (K_i) (µM)	vdW+ bond+ desolv energy (kcal/mol)	Electrostatic Energy (kcal/mol)	Total intercooled Energy (kcal/mol)	Interact surface
(1)	-4.70	298.26	-6.13	-0.07	-6.20	681.133
(2)	-4.81	360.44	-6.15	+0.00	-6.14	721.934

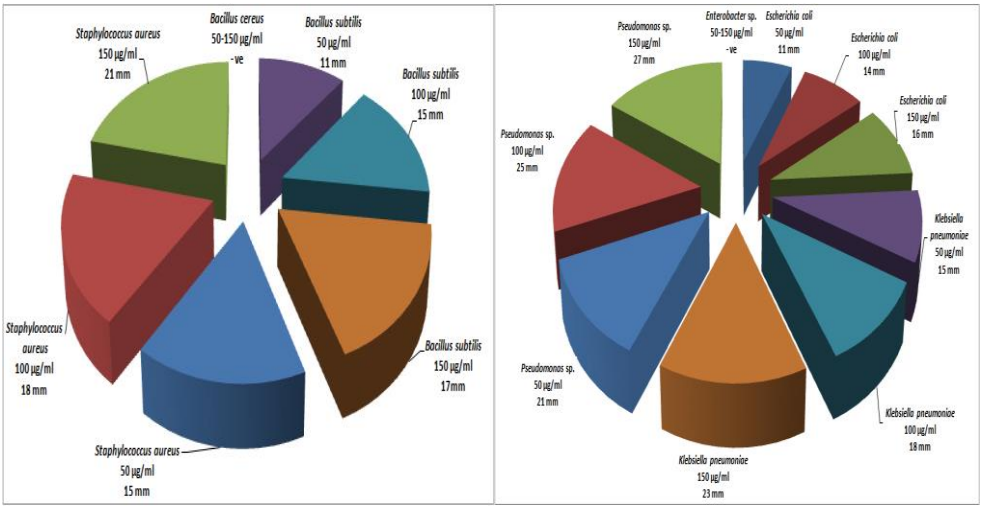

Fig. 7. Antibacterial activity data of compound (1) against gram-positive bacteria (*Bacillus subtilis*, *Staphylococcus aureus* and *Bacillus cereus*) and gram-negative bacteria (*Klebsiella pneumoniae*, *Escherichia coli*, *Pseudomonas* sp. and *Enterobacter* sp.).

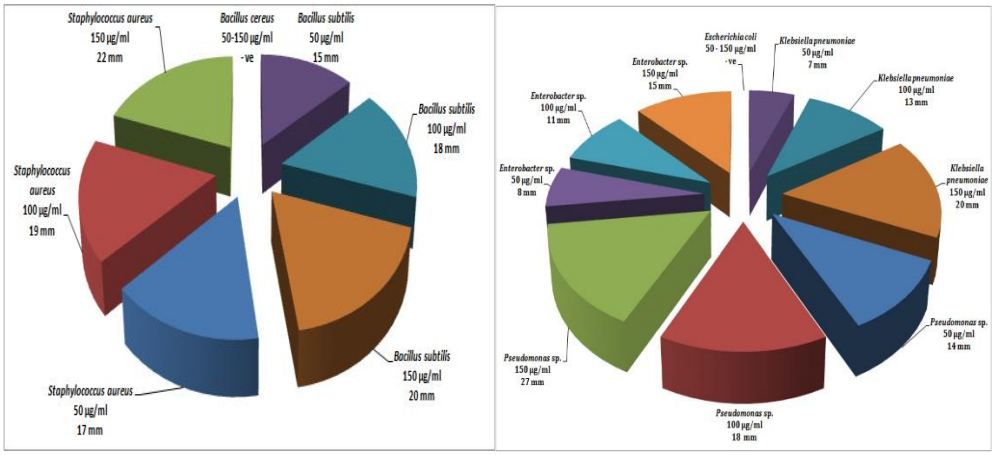

Fig. 8. Antibacterial activity data of compound (2) against gram-positive bacteria (*Bacillus subtilis*, *Staphylococcus aureus* and *Bacillus cereus*) and gram-negative bacteria (*Klebsiella pneumoniae*, *Escherichia coli*, *Pseudomonas* sp. and *Enterobacter* sp.).

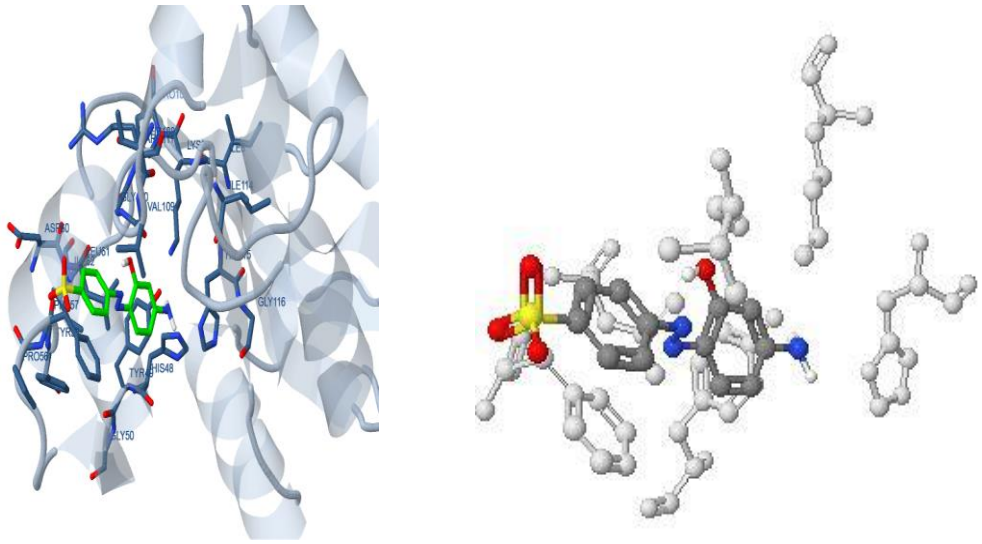

a b

Compound (1)

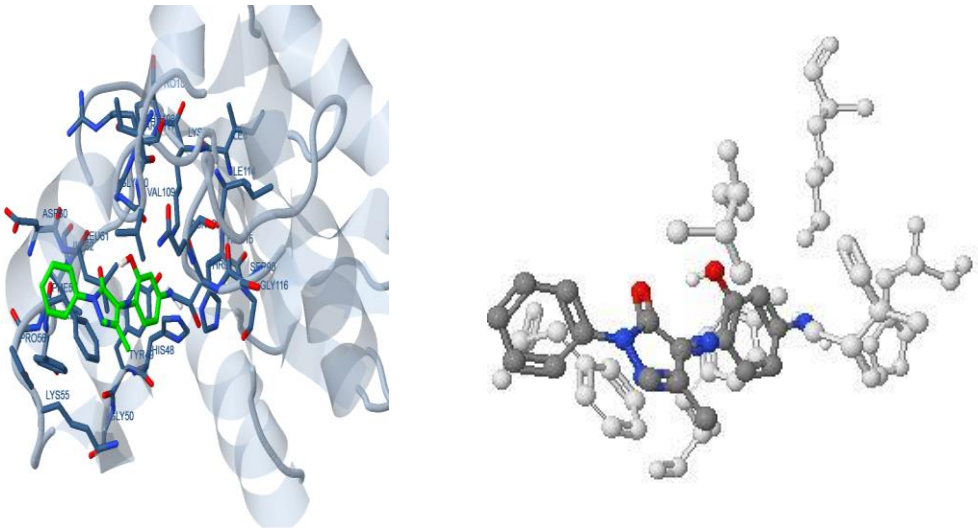

a b

Compound (2)

Fig. 9. The compounds (1 and 2) (green in (a) and gray in (b)) in interaction with receptor of Staphylococcus aureus (3q8u).

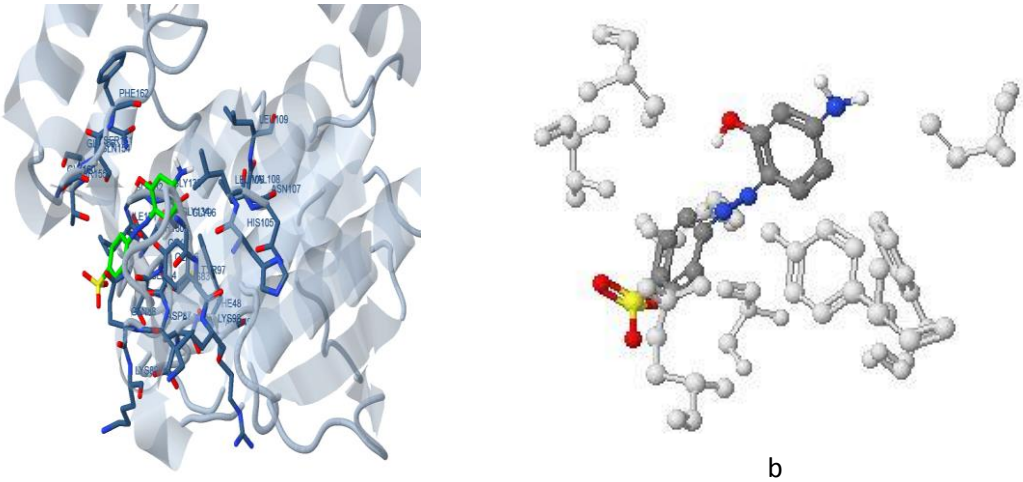

a b

Compound (1)

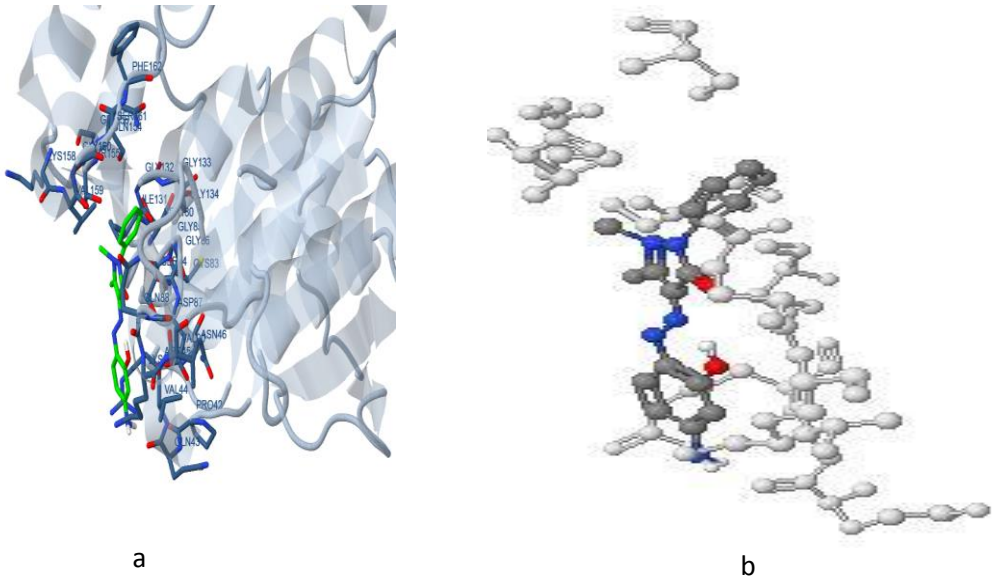

a b

Compound (2)

Fig. 10. The compounds (1 and 2) (green in (a) and gray in (b)) in interaction with receptor of *Escherichia coli* (3t88).

Conclusion

- The inhibition effect of newly synthesized aminophenol derivatives (1 and 2) on C-steel in (2 M HCl) acidic medium were investigated by several electrochemical techniques
- The inhibitive efficiency of C-steel depends on the nature and type of the inhibitor molecule.
- EFM was used as a rapid and nondestructive technique for corrosion measurements.
- The results of EIS revealed an increase in the charge transfer resistance and the decrease in double layer capacitances using EIS technique when the inhibitor is added gave an increase in % IE attributed to the increase of the thickness of the electrical double layer.
- Potentiodynamic polarization technique indicated that the investigated derivatives are mixed-type inhibitors.
- SEM-EDX images and analyses obtained in the presence of synthesized aminophenol derivatives (1 and 2) revealed the formation of thin film on the surface of C-steel.
- All electrochemical measurements were in good agreement.
- The order of % IE of these investigated compounds obey the following order: compound (2) > compound (1).
- The compound (2) showed best interaction with *Staphylococcus aureus* (3q8u) receptor than the compound (1).

- The results showed that the compound (2) is very good antibacterial agents against *Bacillus subtilis* and *Staphylococcus aureus*. The compound (2) is more active than the compound (1) and penicillin G against *Bacillus subtilis* and *Staphylococcus aureus*. It was found that the compound (2) is more active than penicillin G which is used as the antibacterial standard drug against *Enterobacter* sp. and *Klebsiella pneumoniae*.

Acknowledgement

The authors would like to thank Prof. Dr. M.I. Abou-Dobara, Professor of Microbiology, Botany Department, Faculty of Science, Damietta University, Damietta, Egypt for his help during testing antimicrobial activity.

Also, The authors would like to thank Dr. A.M. Eldesoky, Associate professor of Engineering Chemistry Department, High Institute of Engineering &Technology (New Damietta), Egypt and Al-Qunfudah Center for Scientific Research (QCSR), Al-Qunfudah University College, Umm Al-Qura University, KSA, for his help during the study of corrosion inhibition.

Conflicts of interest

The authors declare that they have no conflict of interest.

Appendix A: Supplementary material

See the attached file.

References

[1] Finšgar M., & Milošev I., Inhibition of copper corrosion by 1,2,3-benzotriazole: A review, *Corros. Sci.*, **52**, 2737–2749 (2010).

[2] Eldesoky A. M., El-Bindary M. A., El-Sonbati A. Z., & Morgan Sh. M., New eco-friendly corrosion inhibitors based on azo rhodanine derivatives for protection copper corrosion, *Journal of Materials and Environmental Science* **6** (8), 2260-2276 (2015).

[3] Kokalj, Peljhan S., Finšgar M., & Milošev I., Ab initio modeling of the bonding of benzotriazole corrosion inhibitor to reduced and oxidized copper surfaces, *J. Am. Chem. Soc.*, **132**, 16657–16668 (2010).

[4] Deng S., Li X., & Fu H., Nitrotetrazolium blue chloride as a novel corrosion inhibitor of steel in sulfuric acid solution, *Corros. Sci.*, **52**, 3840–3846 (2010).

[5] Liu F. G., Du M., Zhang J., & Qiu M., Electrochemical behavior of Q235 steel in saltwater saturated with carbon dioxide based on new imidazoline derivative inhibitor, *Corros. Sci.*, **51**, 102-109 (2009).

[6] Musa A. Y., Kadhum A. A. H., Mohamad A. B., & Takriff M.S., The antioxidant activity of new coumarin derivatives, *Corros. Sci.*, **52**, 3331-3340 (2010).

[7] Khaled K. F., & Amin M.A., Polarization curves measurement was used to evaluate corrosion rate of mild steel, *Corros. Sci.*, **51**, 1964-1975 (2009).

[8] El-Sonbati A. Z., Diab M. A., Eldesoky A. M., Morgan Sh. M., & Salem O. L., Polymer complexes. LXXVI. Synthesis, characterization, CT-DNA binding, molecular docking and thermal studies of sulfoxine polymer complexes, *Appl. Organometal. Chem.*, 33, e4839 (2019).

[9] El-Sonbati A. Z., Diab M. A., Morgan Sh. M., Eldesoky A. M., & Balboula M. Z., Polymer complexes. LXIX. Some divalent metal (II) polymer complexes of potentially bidentate monomer N-[4-(5-methyl-isoxazol-3-ylsulfamoyl)-phenyl]-acrylamide: Synthesis, spectroscopic characterization, thermal properties, antimicrobial agents and DNA studies, *Appl. Organometal.Chem,*. **32**, e4207 (2018).

[10] Abou-Dobara M. I., Omar N. F., Diab M. A., El-Sonbati A. Z., Morgan Sh. M., Salem O. L., & Eldesoky A., Polymer complexes. LXXV. Characterization of quinoline polymer complexes as potential bio-active and anti-corrosion agents, *Mater. Sci. Eng. C*, **103**, 109727 (2019).

[11] El-Sonbati A. Z., El-Bindary A. A., Mohamed G. G., Morgan Sh. M., Hassan W. M. I., & Elkholy A.K., Geometrical structures, thermal properties and antimicrobial activity studies of azodye complexes, *J. Mol. Liq.*, **218**, 16–34 (2016).

[12] Morgan Sh. M., Diab M. A., & El-Sonbati A. Z., Synthesis, spectroscopic, thermal properties, Calf thymus DNA binding and quantum chemical studies of M (II) complexes, *Appl. Organometal.Chem.*, **32**, e4281 (2018).

[13] Morgan Sh. M., Diab M. A., & El-Sonbati A. Z., Synthesis, molecular geometry, spectroscopic studies and thermal properties of Co (II) complexes, *Appl. Organometal.Chem.*, **32**, e4305 (2018).

[14] Abou-Dobara M. I., El-Sonbati A. Z., & Morgan Sh. M., Influence of substituent effects on spectroscopic properties and antimicrobial activity of 5-(4′-substituted phenylazo)-2-thioxothiazolidinone derivatives, *World J. Microbiol. Biotechnol.*, **29**, 119-126 (2013).

[15] Abou-Dobara M. I., Omar N. F., Diab M. A., El-Sonbati A. Z., Morgan Sh. M., & El-Mogazy M. A., Allyl rhodanine azo dye derivatives: Potential antimicrobials target d-alanyl carrier protein ligase and nucleoside diphosphate kinase, *J. Cell. Biochem.*, **120**, 1667-1678 (2019).

[16] Refaat H. M., El-Badway H. A., & Morgan Sh. M., Molecular docking, geometrical structure, potentiometric and thermodynamic studies of moxifloxacin and its metal complexes, *J. Mol. Liq.*, **220**, 802-812 (2016).

[17] Mohamed G. G., El-Sherif A. A., Saad M. A., El-Sawy S. E., & Morgan Sh. M., Mixed-ligand complex formation of tenoxicam drug with some transition metal ions in presence of valine: Synthesis, characterization, molecular docking, potentiometric and evaluation of the humeral immune response of calves, *J. Mol. Liq.*, **223**, 1311-1332 (2016).

[18] Diab M. A., Mohamed G. G., Mahmoud W., El-Sonbati A. Z., Morgan Sh. M., & Abbas S. Y., Inner metal complexes of tetradentate Schiff base: Synthesis, characterization, biological activity and molecular docking studies, *Appl. Organometal. Chem.*, **33**, e4945 (2019).

[19] El-Sonbati A. Z., Diab M. A., Morgan Sh. M., & Seyam H. A., Supramolecular structures for determination and identification of the bond lengths in novel uranyl complexes from their infrared spectra, *J. Mole. Struct.*, **1154**, 354-365 (2018).

[20] El-Sonbati A. Z., Mahmoud W., Mohamed G. G., Diab M. A., Morgan Sh. M., & Abbas S. Y., Synthesis, characterization of Schiff base metal complexes and their biological investigation, *Appl. Organometal. Chem.*, **33**, e5048 (2019).

[21] Morgan Sh. M, Diab M. A, & El-Sonbati A. Z., Supramolecular assembly of hydrogen bonding, ESR studies and theoretical calculations of Cu (II) complexes *Appl. Organometal. Chem.*, **32**, e4504 (2018).

[22] El-Sonbati A. Z., Diab M. A., Mohamed G. G., Saad M. A., Morgan Sh. M., & El-Sawy S. E. A., Polymer complexes. LXXVII. Synthesis, characterization, spectroscopic studies and immune response in cattle of quinoline polymer complexes, *Appl. Organometal. Chem.*, **33**, e4973 (2019).

[23] Diab M. A., Nozha S. G., El-Sonbati A. Z., El-Mogazy M. A., & Morgan Sh. M., Polymer complexes. LXXVIII. Synthesis and characterization of supramolecular uranyl polymer complexes: Determination of the bond lengths of uranyl ion in polymer complexes, *Appl. Organometal. Chem.*, **33**, e5153 (2019).

[24] Morgan Sh. M., El-Ghamaz N. A., & Diab M. A., Effect of the type of metal on the electrical conductivity and thermal properties of metal complexes: The relation between ionic radius of metal complexes and electrical conductivity, *J. Mol. Struct.*, **1160**, 227-241 (2018).

[25] El-Ghamaz N. A., El-Sonbati A. Z., & Morgan Sh. M., Optical properties of some synthesized azo thin films, *J. Mol. Struct.*, **1027**, 92-98 (2012).

[26] El-Ghamaz N. A., Diab M. A., El-Sonbati A. Z., Morgan Sh. M., & Salem O. L., Polymer complexes. LXVII: electrical conductivity and thermal properties of polymer complexes of quinoline azo dye, *Chem. Pap.*, **71**, 2417-2433 (2017).

[27] El-Sonbati A. Z., Belal A. A., El-Gharib M. S., & Morgan Sh. M., Supramolecular structure, mixed ligands and substituents effect on the spectral studies of oxovanadium (IV) complexes of bioinorganic and medicinal relevance. *Spectrochim. Acta A*, **95**, 627-636 (2012).

[28] El-Sonbati A. Z., Diab M. A., Belal A. A. M., & Morgan Sh. M., Supramolecular structure and spectral studies on mixed-ligand complexes derived from β-diketone with azodye rhodanine derivatives, *Spectrochim. Acta A*, **99,** 353-360 (2012).

[29] Ravichandran R., & Rajendran N., Electrochemical behaviour of brass in artificial seawater: effect of organic inhibitors, *Appl. Sur. Sci.*, **241**, 449-458 (2005).

[30] Ravichandran R., & Rajendran N., Influence of benzotriazole derivatives on the dezincification of 65–35 brass in sodium chloride, *App. Sur. Sci.*, **239**, 182-192 (2005).

[31] Al-Khaldi M. A., & Al-qahtani K. Y., Corrosion inhibition of steel by Coriander extracts in hydrochloric acid solution, *J. Mater. Environ. Sci.*, **4**, 593-600 (2013).

[32] Samie F., Tidblad J., Kucera V., & Leygraf C., Effect of Carbon Dioxide on Sodium Chloride-Induced Atmospheric Corrosion of Copper, *Atmospheric Environ.* **39**, 7362-7373 (2005).

[33] Silverman D. C., & Carrico J. E., Electrochemical Impedance Technique — A Practical Tool for Corrosion Prediction, *Corrosion*, **44**, 280-287 (1988).

[34] Macdonald D. D., & Mckubre M. C. H., "Impedance measurements in electrochemical systems" Modern Aspects of Electrochemistry, (Bockris J. O'M., Conway B. E., White R. E., Eds., Plenum Press, New York, pp.61–150 (1982).

[35] Mansfeld F., Recording and Analysis of AC Impedance Data for Corrosion Studies, *Corrosion*, **36**, 301-307 (1981).

[36] Gabrielli C., "Identification of Electrochemical processes by Frequency Response Analysis" (Solarton Instrumentation Group) (1980).

[37] Anejjar A., Zarrouk A., Salghi R., Zarrok H., Ben Hmamou D., Hammouti B., Elmahi B., & Al-Deyab S.S., Studies on the Inhibitive Effect of the Ammonium Iron (II) Sulphate on the Corrosion of Carbon Steel in HCl Solution, *J. Mater. Environ. Sci.*, **4**, 583-592 (2013).

[38] Kus E., & Mansfeld F., An evaluation of the electrochemical frequency modulation (EFM) technique, *Corros. Sci.*, **48**, 965-979 (2006).

[39] Silverman D.C., & Carrico J.E., Electrochemical. Impedance Technique — A Practical Tool for. Corrosion Prediction, *Nat. Assoc. Corros. Engin.*, **44**, 280-287 (1988).

[40] Moretti G., Quartanone G., Tassan A., & Zingales A., Inhibition Effects of Some Schiff's Bases on the Corrosion of Mild Steel in Hydrochloric Acid Solution, *Wekst. Korros.*, **45**, 641-647 (1994).

[41] Issa R. M., Awad M. K., & Atlam F. M., Quantum chemical studies on the inhibition of corrosion of copper surface by substituted uracils, *Appl. Surf. Sci.***, 255**, 2433-2441 (2008).

[42] Khaled K.F., Preparation and characterization of titanate nanotubes/carbon composites, *Mater. Chem. phys.*, **112**, 290-300 (2008).

[43] Morgan Sh. M., El-Sonbati A. Z., & El-Mogazy M. A., Polymer complexes. LXX. Synthesis, spectroscopic studies, thermal properties and antimicrobial activity of metal (II) polymer complexes, *Appl. Organometal. Chem.*, **32**, e4264 (2018).

[44] Morgan Sh. M., El-Sonbati A. Z., & Eissa H. R., Geometrical structures, thermal properties and spectroscopic studies of Schiff base complexes: Correlation between ionic radius of metal complexes and DNA binding, *J. Mol. Liq.*, **240**, 752-776 (2017).

[45] El-Sonbati A. Z., Diab M. A., Morgan Sh. M., & Balboula M. Z., Polymer complexes. LXVIII. Spectroscopic studies of supramolecular copper

(II) polymeric complexes of biologically active monomer derived from novel sulfa drug, *Appl. Organometal.Chem.*, **32**, e4059 (2018).

[46] Habib N. S., Rida S. M., Badawey E. A. M., Fahmy H. T. Y., & Ghozlan H. A., Synthesis and antimicrobial activity of rhodanine derivatives, *Eur. J. Med. Chem,*. **32**, 759-762 (1997).

[47] Diab M. A., El-Sonbati A. Z., Morgan Sh. M., El-Mogazy M. A., Polymer complexes. LXXI. Spectroscopic studies, thermal properties, DNA binding and antimicrobial activity of polymer complexes, *Appl. Organometal. Chem.,* **32**, e4378 (2018).

[48] El-Sonbati A. Z., Diab M. A., Morgan Sh. M., & El-Mogazy M. A., Polymer complexes. LXXIII. Synthesis, characterization, thermal properties, electron spin resonance study and antimicrobial activity of Cu (II) polymer complexes: Relation between representative Pascal constants and thermal activation energy of decomposition, *Appl. Organometal. Chem.,* **32**, e4530 (2018).

[49] El-Sonbati A. Z., Diab M. A., & Morgan Sh. M., Thermal properties, antimicrobial activity and DNA binding of Ni (II) complexes of azo dye compounds, *J. Mol. Liq*., **225**, 195-206 (2017).

[50] El-Sonbati A. z., Diab M. A., Morgan Sh. M., Abou-Dobara M. I., & El-Ghettany A. A., Synthesis, characterization, theoretical and molecular docking studies of mixed-ligand complexes of Cu (II), Ni (II), Co (II), Mn (II), Cr (III), UO_2 (II) and Cd (II), , *J. Mol. Struct*., **1200,** 127065 (2020).

[51] Nozha S. G., Morgan Sh. M., Abu Ahmed S. E., El-Mogazy M. A., Diab M. A., El-Sonbati A. Z., Abou-Dobara M. I., Polymer complexes. LXXIV. Synthesis, characterization and antimicrobial activity studies of polymer complexes of some transition metals with bis-bidentate Schiff base, *J. Mol. Struct.,* **1227,** 129525 (2021).